UNIVERSITAT POLITÈCNICA DE CATALUNYA
BARCELONATECH
Facultat d'Informàtica de Barcelona

hola

New real-time GNSS algorithms for detection and measurement of potential geoeffective stellar flares

Author
David Moreno Borràs

Supervisor
Manuel Hernández-Pajares

Specialization
Computing

April 5, 2019

Abstract

Solar flares are sudden electromagnetic emissions on the Sun's surface that release large amounts of magnetic energy. These flares emit radiation that has an effect on Earth's ionosphere electron content and are detected by telescopes such as Swift or Fermi by performing gamma-ray observations from low Earth orbit. (Swift y fermi no son para solar flares son para GRB en general!!, quizas aqui deberia ir alguno que se centre en el sol especificamente)

Another approach for detecting these events is possible: the ionosphere electron content variation can be studied using data from the Global Navigation Satellite System (GNSS), specifically the Global Positioning System (GPS).....????

Algorithms for detecting solar flares without knowing the location of the source, that is, the position of the Sun relative to Earth, as well as a study on the feasibility of the detection of such events for the challenging scenario of far-away stars, are presented, aiming to find an alternative detection method to that of the telescopes and using free, open-source data.

Keywords: Solar flares, stellar flares, algorithms, GNSS, GPS, IGS, gamma ray bursts?

Contents

1 GEP **5**

2 Background **6**
2.1 Global Navigation Satellite Systems 6
2.2 Ionosphere 7
2.3 Stellar flares 7
2.4 Gamma-Ray Bursts 8

3 Study on the feasibility of stellar flare detection **9**
3.1 Sources of data and possible candidates 9
3.2 The Neil Gehrels Swift Observatory and its data 10
3.3 Objective function 11
3.4 Obtaining the data 12
3.5 Results 13

4 Solar flare detection **14**
4.1 Data 14
4.1.1 GPS Data 14
4.1.2 The Halloween Storm 15
4.1.3 Formatting 15
4.1.4 AWK 16
4.2 VTEC 16
4.2.1 Computing the VTEC 16
4.2.2 Distribution throughout the day 16
4.3 Solar-zenith angle 18
4.4 Results 20

5 Sun flare detection algorithm **21**
5.1 Key elements 21
5.1.1 Correlation 21
5.1.2 Moment of the flare 21
5.2 Brute force approach 21
5.2.1 Pseudocode 21
5.2.2 Linking C++ and Fortran 22
5.2.3 Results 23

Listings

3.1 Python function for computing the angle 12
4.1 process 16
4.2 Bash script to execute the procedures 17
4.3 Reading the content of the file and storing the computations for plotting . . 19
4.4 Computation of the solar-zenith a angle 19
5.1 Python example 22
5.2 Brute force approach algorithm output 23

List of Figures

4.1 VTEC distribution throughout the day for all IPPS (a) and for IPPs that have Vill as the receiver (b) 18
4.2 VTEC value as a function of the solar-zenith angle cosine 20
4.3 VTEC value as a function of the solar-zenith angle cosine 20

5.1 dasdasdasda 22

- Cover
- ListOfContents
- ListOfFigures???
- ListOfListings???
- Abstract/Resumen/Resum

Content

- ch1 GEP
- ch2 Background/Introduction
  - Global Navigation Satellite Systems
  - Ionosphere
  - Stellar flares
  - Gamma-Ray Bursts
- ch3 Study on the feasiblity of stellar flare detection (far-away stars)
  - Sources of data and possible candidates
  - The Neil Gehrels Swift Observatory and its data
  - Objective function
  - Obtaining the data
  - Results
- ch4 Solar flare detection
  - Data
    - GNSS Data
    - The Halloween Storm
    - Formatting
    - AWK
  - Vtec distribution
  - Algorithm
  - Results
- ch5 Solar flare detection: Unknown location (nombre del algoritmo aqui)
  - First approach: Brute force
  - Hill Climbing bla bla

Annexes

- Glossary (Acronyms)
- References

Chapter 1

GEP

merda del gep

Chapter 2

Background

As the project has a large background in physics and astronomy, some of the relevant topics that are going to be studied are introduced: Global Navigation Satellite Systems, the Ionosphere, Stellar Flares and Gamma-Ray Bursts.

2.1 Global Navigation Satellite Systems

GNSS and GPS

These two terms may lead to confusion as Global Navigation Satellite Systems (GNSS) is the generic term for all satellite navigation systems. The Global Positioning System (GPS), in particular, is the United States' GNSS system, the world's most used one. Other systems, for example, are the European Galileo or Russian GLONASS [7].

Global Navigation Satellite Systems use satellites to determine the position of a given object or device in terms of latitude, longitude and height.

Positioning

In short, GNSS works as follows: out of all the GNSS satellites orbiting Earth, at least four of them are constantly visible from a specific point and transmitting information at a certain frequency. When a device receives a signal from one of them, the distance to the satellite can be calculated by means of the time required to reach it and the speed of light. As many variables might affect the speed of light such as the medium through which it is propagating, this estimation of the distance is called **pseudo-range**.

Thus, the location of the receiver can be estimated using a technique called **trilateration**. Having three spheres around each of the satellites with the pseudo-range as their radius, the intersection of these spheres yields the location of the receiver [11].

Ionospheric Piercing Points

Ionospheric Piercing Points (IPP) are going to be very relevant throughout the development of the project is dsadasdasd

The International GNSS Service

In 1998 the International GNSS Service (IGS) was created as a collaboration of several members of the scientific community: Center for Orbit Determination in Europe (CODE), (European Space Agency) ESA, Jet Propulsion Laboratory (JPL) and Polytechnic University of Catalonia (UPC). This voluntary federation has made available open access GNSS data since its creation [2] [4].

Its data is provided by more than 300 GPS receivers around the globe and is processed by the previous institutions which compute the global distribution of the Total Electron Content (TEC) [9].

GNSS is a key component to this project because, as mentioned before, many variables can affect the speed of light and therefore the time it takes for the transmitter's signal to be intercepted by the receiver. One of these variables is the electron content of the layer of the atmosphere where GNSS satellites operate: the ionosphere.

2.2 Ionosphere

The ionosphere is a layer of the Earth's atmosphere that lies 75-1000km above the surface of the planet [19].

High energy from Extreme UltraViolet (EUV) and X-ray radiation can cause its atoms to be ionized and create a layer of electrons [16]. Due to these free electrons and ionized molecules, it is capable of affecting radio wave propagation, thus having an effect on Global Navigation Satellite Systems (GNSS) technology, this phenomena allows these satellites to be used as a global scanner for the ionosphere [10].

The main physical quantity used for describing the electron content of the ionosphere is the **Total Electron Content (TEC)**, the TEC is the total number of electrons between two points $(r1, r2)$ along a cylinder of base $1m^2$. Slant TEC (STEC), in particular, can be defined as the TEC in which $r1$ and $r2$ are a satellite and a receiver's positions [18].

The unique properties the ionosphere has enable us to use the data provided by the GNSS technology to study a powerful phenomena that occurs in many stars across the universe: stellar flares.

2.3 Stellar flares

Flares from stars, in particular those that have the Sun as a source, more noticeable due to its proximity, are sudden flashes of brightness in the surface of stars which release large amounts of energy across the whole electromagnetic spectrum[1]. Flares that have the Sun as a source can increase the electron content of the ionosphere and have an effect on waves passing through it, affecting satellite communications and causing a delay. This phenomena is the key element of the project, as it enables us to study these events.

Satellites can also be harmed by this effects: the flares heat up the outer atmosphere, which in turn increases the drag on these satellites reducing their lifetime in orbit. GPS

[1] X-rays and Extreme Ultraviolet (EUV) radiation

as a solar observational instrument: Real-time estimation of EUV photons flux rate during strong, medium, and weak solar flares se explica el efecto del sol sobre ionosfera

The previous phenomena applies to flares originating in the Sun, whether a flare that has a star from outside the Solar System as a source has an effect on the Earth's atmosphere or not is one of the topic that is going to be studied in this project.

SOHO and GOES are space probes used for obtaining solar flare information [8]

2.4 Gamma-Ray Bursts

Throughout the project, in particular when studying the feasibility of stellar flares detection, another type of event will be mentioned and studied as well: Gamma-Ray Bursts (GRBs):

GRBs are highly energetic explosions that occur in distant galaxies, releasing large amounts of radiation, in particular Gamma rays, hence the name of the event. These bursts, despite being millions of light years away from Earth are so powerful they might still have an impact on the ionosphere, like the aforementioned stellar flares. The main difference with flares originating from stars is that GRBs are thought to be originated from the death of massive stars, that is, supernovas.

This event, despite not being a stellar flare, the phenomena we aim to detect, is going to be studied in the following sections to test the currently working algorithms mainly for two reasons: it has been studied and cataloged by telescopes such as the Fermi Observatory and there's is available information that we can use for our study, and the large amounts of energy they emit it make GRBs a more feasible target to detect.

Fermi Observations of High-Energy Gamma-Ray Emission from GRB 080916C

Chapter 3

Study on the feasibility of stellar flare detection

Flares from far-away stars and Gamma-ray Bursts, albeit more powerful than flares that have the Sun as their source, may not be possible to detect due to the large distances that separate them from our measurement tool: the ionosphere.

Before starting to adapt the algorithm for detecting solar flares to this scenario, a study was conducted parallel to its development, to see if the energy from flares originating in far-away stars could be detected using the already existing method, namely the GNSS Solar Flare Activity Indicator (GSFLAI) algorithms [8].

To study if this was feasible, the algorithms were run on certain candidates of flares and GRBs to see if they could be detected.

The project supervisor, Manuel Hernández-Pajares, who as mentioned before has previously performed several studies on the subject, provided the GSFLAI algorithm to test the candidates. The GSFLAI algorithm takes into consideration the location of the source (the Sun) to see if there's a relation between an increase in the VTEC of the ionosphere and the solar-zenith angle to determine if this increase is caused by a solar flare. [GNSS measurement of EUV photons flux rate during strong and mid solar flares]

However, its execution may take up to 2 hours, because of this the aim was to:

- Find a database for possible candidates, several online archives with information about previously recorded Gamma Ray Bursts were considered.
- Select an appropriate source of this pool of candidates by writing a quick script that yielded an ordered list of the best candidates based on certain factors, instead of selecting a random source.

3.1 Sources of data and possible candidates

The three main databases we considered for the study were:

- The GRB collection website of Jochen Greiner, scientist at the Max-Planck-Institute for extraterrestrial Physics (MPE) [13], which offers a collection of detected GRBs by different telescopes and observatories.

- The Magnetar Outburst Online Catalog (MOOC), developed by the Institute of Space Sciences (CSIC-IEEC, Barcelona) [12]. We also had the pleasure to meet one of the leaders of this project, Nanda Rea, and discuss
- The Neil Gehrels Swift Observatory website and archive by the National Aeronautics and Space Administration (NASA), Goddard Space Flight Center [6] which contains an archive of detected GRBs by the Swift observatory and is constantly updated.

Because of the layout of the website and how the data could be accessed, the option with which we started was the Swift Database, as the data could be visualized in an HTML table and was easily accessible.

3.2 The Neil Gehrels Swift Observatory and its data

The Swift Observatory is a NASA mission with international participation, designed to observe GRBs and their afterglows to study topics such as the origins of GRBs or what they can reveal about the early stages of the universe [17]. The observatory is equipped with three main instruments that work with each other to study GRBs [5] [6]:

- The **Burst Alert Telescope (BAT)**, tasked with detecting the GRBs and computing their positions. This triggers the spacecraft to point the other telescopes to the burst so it can be studied in more detail.
- The **X-ray Telescope (XRT)**, used for studying the X-ray radiation and taking images of the bursts which in turn help increase the accuracy of the location estimation.
- The **UV/Optical Telescope (UVOT)**, which serves a similar purpose to the XRT, but studies the ultraviolet band of the spectrum.

For each detected GRB, the data obtained by the different telescopes is given. The parameters that are relevant to our study and determine the fitness of each of the candidates are:

- The **name of the burst**, given by the date it was detected. For example, the GRB named 190220A was detected the 20th of February of 2019.
- The **Universal Time (UT)** of the detection, that is, hh:mm:ss of the day given by the name.
- The fluence detected by the BAT component, in units of keV. that is.
- The **UVOT magnitude**, measured by the UV Telescope.
- The location that triggered the detection, given as **Right Ascension (Ra)** and **Declination (Dec)**.

Right Ascension and Declination are two concepts similar to longitude and latitude, respectively, used to describe the location of objects in the sky, in particular in a sphere of infinite radius that with the Earth as its center called the **celestial sphere**.

Taking this into account, Right Ascension is the equivalent of longitude, expressed in degrees (or more commonly in hours, minutes and seconds) and Declination, the equivalent of latitude, is expressed in degrees between the two poles: +90º and -90º. [20]

This reference system is used to describe the position of objects in the sky, and it is the one used by the Swift telescope to specify the location of the sources. Afterwards these concepts will play an important role when computing the angle formed between the source and the Sun.

3.3 Objective function

Our main goal in this section was to obtain a list of GRB candidates ordered from more to less probable to be detected by the algorithm, that is, their fitness. To obtain this score we had to define an objective function, taking into consideration two factors:

- The **strength** of the burst, given by the UVOT magnitude. If this value was not available (as it was the case with many of the candidates) the BAT fluence was considered as its strength. This values were already given by the archive and no additional computations were required.
- The **angle between the burst and the Sun**, this was an important factor because bursts having an effect on the night hemisphere should be more noticeable than those hitting the day one, where the Sun has a bigger influence.

Computing the angle

As mentioned before, the Swift archive gives us the Right Ascension (Ra) and Declination (Dec) where the source is thought to be located.

The location of the Sun, on the other hand, is unknown. But we do know the time when the burst was detected.

The supervisor, Manuel Hernández-Pajares, provided me an algorithm which takes date (year, month, day and UT) and a planet of the Solar System (or the Sun, our case) as the input and returns its location in the celestial sphere, that is, its Ra and Dec.

This algorithm belongs to the **Starlink Project** (Rutherford Appleton Laboratory), which provided open-source software like the one at hand to astronomical institutions. Although it was shut down in 2005, the code still remains and we could use it for our study [1].

Knowing the location of the GRB: (δ_g, α_g), declination and right ascension, respectively. And that of the Sun: (δ_s, α_s), the cosine of the angle between both can be computed and used as a parameter for the objective function.

This computation is done by performing the dot product of the two unit vectors that can be obtained from the Ra and Dec of the objects given by the following formulas: [**?**] TODO: arreglar esta cita

$$unitVectorGRB = \begin{bmatrix} \cos\delta_g * \cos\alpha_g \\ \cos\delta_g * \sin\alpha_g \\ \sin\delta_g \end{bmatrix} \tag{3.1}$$

$$unitVectorSun = \begin{bmatrix} \cos\delta_s * \cos\alpha_s \\ \cos\delta_s * \sin\alpha_s \\ \sin\delta_s \end{bmatrix} \tag{3.2}$$

$$\cos angleSunGRB = unitVectorGRB \cdot unitVectorSun \tag{3.3}$$

The code for the previous computation is shown here:

```
def scorePosition(sunRa, sunDec, ra, dec):
  # If Ra and/or Dec are n/a, return 0, else, compute the dotProduct
   if ra == 0 or dec == 0:
     return 0

   coordSun = [math.cos(sunDec)*math.cos(sunRa),
   math.cos(sunDec)*math.sin(sunRa),
   math.sin(sunDec)]

   coordGRB = [math.cos(dec)*math.cos(ra),
    math.cos(dec)*math.sin(ra),
     math.sin(dec)]

   angle = math.acos(coordSun[0]*coordGRB[0] +
   coordSun[1]*coordGRB[1] +
   coordSun[2]*coordGRB[2])

   angle = angle*180/math.pi

   return angle
```

Listing 3.1: Python function for computing the angle

3.4 Obtaining the data

Regarding the scrapping of the website to parse the data and obtain this ordered list, **Python** was chosen because the problem required a quick implementation, and Python's libraries offered a great tool to develop a simple solution as quick as possible.

In the script, the website with the table of bursts (see figure x) is scrapped using Python's **BeautifulSoup** library, which has an HTML and XML parser that allows us to easily select and obtain data from a given website.

Insertion sort was used so we could insert every considered GRB into a list of sorted candidates as we were traversing the table.

Regarding the distribution of weight between both factors, strength and angle, we ....

The best 10 candidates of the resulting sorted table (pie de pagina: bursts registered up to the 26th of February of 2019), is shown here:

We proceeded to study these bursts

3.5 Results

Chapter 4

Solar flare detection

Before starting to develop the main solar flare detection algorithm a first program was developed that would target a powerful solar flare for which we know the time of the event and therefore, the location of the Sun.

Although the aim of the main algorithm is detecting the solar flare without taking into consideration the position of the Sun, this first approach was done to understand how the inner part of the algorithm works: studying the correlation between the cosine of the solar-zenith angle and the VTEC content.

This sections also provides an introduction to the formatting and use of the Global Navigation Satellite Systems data (GPS in this case) and how the main parameters are computed.

4.1 Data

4.1.1 GPS Data

Since 1992, the CDDIS has supported GNSS data and product archiving for the International GNSS Service (IGS) as one of four global data centers. In this capacity, the CDDIS provides online access to the GNSS data generated by the IGS network as well as the IGS standard, working group, and pilot project products derived from these data.

Hablar de donde salen, el fichero ti me lo ha dado manuel. El fichero ti es el resultado de "pre-procesar" los datos Raw que hay en la web de ftp://cddis.nasa.gov/.

[3] -¿ The Crustal Dynamics Data Information System (CDDIS) was initially developed to provide a central data bank for NASA's Crustal Dynamics Project (CDP). The system continues to support the space geodesy and geodynamics community through NASA's Space Geodesy Project as well as NASA's Earth Science Enterprise. The CDDIS was established in 1982 as a dedicated data bank to archive and distribute space geodesy related data sets. Today, the CDDIS archives and distributes mainly Global Navigation Satellite Systems (GNSS, currently Global Positioning System GPS and GLObal NAvigation Satellite System GLONASS), laser ranging (both to artificial satellites, SLR, and lunar, LLR), Very Long Baseline Interferometry (VLBI), and Doppler Orbitography and Radio-positioning Integrated by Satellite (DORIS) data for an ever increasing user community of geophysists.

The CDDIS is operational on a dedicated computer located at the Goddard Space Flight Center in Greenbelt, MD. The CDDIS has served as a global data center for the International GNSS Service (IGS) since 1992. The CDDIS also actively supports the International Laser Ranging Service (ILRS), the International VLBI Service for Geodesy and Astrometry (IVS), International DORIS Service (IDS), and the International Earth Rotation and Reference Systems Service (IERS) as a global data center. To learn more about these space geodetic techniques and their respective CDDIS data holdings, click on the images below.

[15] -¿ Since 1982, the Crustal Dynamics Data Information System (CDDIS) has supported the archive and distribution of geodetic data products acquired by the National Aeronautics and Space Administration (NASA) as well as national and international programs. The CDDIS provides easy, timely, and reliable access to a variety of data sets, products, and information about these data. These measurements, obtained from a global network of nearly 650 instruments at more than 400 distinct sites, include DORIS (Doppler Orbitography and Radiopositioning Integrated by Satellite), GNSS (Global Navigation Satellite System), SLR and LLR (Satellite and Lunar Laser Ranging), and VLBI (Very Long Baseline Interferometry). The CDDIS data system and its archive have become increasingly important to many national and international science communities, particularly several of the operational services within the International Association of Geodesy (IAG) and its observing system the Global Geodetic Observing System (GGOS), including the International DORIS Service (IDS), the International GNSS Service (IGS), the International Laser Ranging Service (ILRS), the International VLBI Service for Geodesy and Astrometry (IVS), and the International Earth rotation and Reference frame Service (IERS). Investigations resulting from the data and products available through the CDDIS support research in many aspects of Earth system science and global change. Each month, the CDDIS archives more than one million data and derived product files totaling over 90 Gbytes in volume. In turn, the global user community downloads nearly 1.2 Tbytes (over 10.5 million files) of data and products from the CDDIS each month. The requirements of analysts have evolved since the start of the CDDIS; the specialized nature of the system accommodates the enhancements required to support diverse data sets and user needs. This paper discusses the CDDIS, including background information about the system and its user communities, archive contents, available metadata, and future plans.

Explicar que es cddis, como se procesan los datos, link al [9], ahi esta explicado como los procesa

For this section, only these pre-processed Ti files were needed, as detecting the flares in real time is a task that will be discussed later in the project.

4.1.2 The Halloween Storm

To test this, the data used was that of the called "Hallowen Storm, in which

Halloween storm, poner ejemplos, citar al texto, porque esta tormenta otros papers de la storm tambien, decir que usaremos el momento exacto 11.05

4.1.3 Formatting

hablar de los datos, el formato, relevant to this algorithm: mappingion, d2li, etc

4.1.4 AWK

Usaremos awk, como va, muy breve

With this data we can obtain the two parameters that will yield the previously shown plot: the VTEC value and the cosine of the solar-zenith angle

4.2 VTEC

Fisrt we wanted to obtain VTEC distribution throughout the day, to visually see if any spikes appeared confirming that the moment we were going to study based on the paper [8] was correct.

For each epoch in our data set (from 10.5 to 11.5 with a sampling rate of 30 seconds) we needed to compute de VTEC value.

4.2.1 Computing the VTEC

The VTEC can be estimated using the following approach:

bla bla bla justify the following equation

$$\frac{d^2V}{dt^2} = \frac{d^2Li}{M} \tag{4.1}$$

Where $M = \frac{1}{\cos Z}$ is the "ionospheric mapping function", given by the inverted cosine of the satellite-zenith angle that we have for each IPP. [8]

Therefore, we can estimate the VTEC of an IPP by dividing two of the given fields in the data file:

$$VTEC \approx \frac{d^2Li}{M} \tag{4.2}$$

The Vtec...formulas...d2li/mappingio

4.2.2 Distribution throughout the day

Because the only operation that had to be performed was the previous division, a simple AWK script was used to filter out the two necessary fields from the data file (d2li and mapping) and print the resulting value and the time.

```
{
  /a/
  d2li = $21;
  mappingFunc = $43;
  vtec = d2li/mappingFunc;
  print $3 " " vtec
}
```

Listing 4.1: process

```
#!/bin/bash
tiDataFile="../data/ti.2003.301.10h30m-11h30m.gz"

zcat "$tiDataFile" | gawk -f previewVTECDistribution.awk > vtecValues
gnuplot -e "set terminal png; set output 'vtecDistribution.png'; set title '
    VTEC Distribution'; set xlabel 'Time of the day (hours)'; set ylabel 'VTEC
    '; set grid; plot \"vtecValues\" using 1:2 with point"
rm vtecValues
```

Listing 4.2: Bash script to execute the procedures

The bash script executes the AWK process with the data as the input and outputs n rows with two columns: the time of the day and the calculated VTEC, plotting the results using Gnuplot. The results can be seen in figure 4.1, where we can see how the VTEC value evolves throught the day. Visually, a spike can be seen between 11 and 11.2 hours.

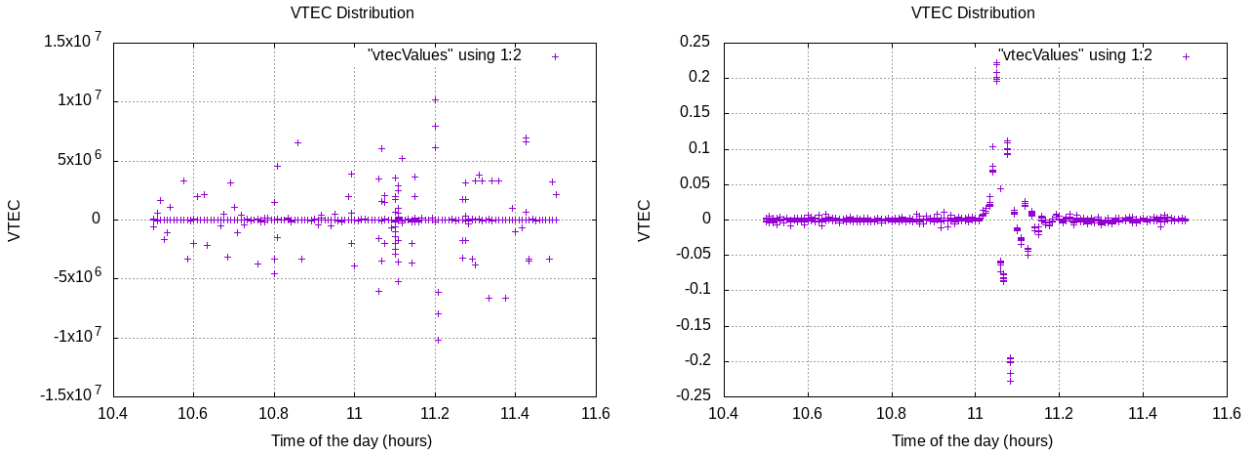

(a) All IPPs

(b) Villafranca station

Figure 4.1: VTEC distribution throughout the day for all IPPS (a) and for IPPs that have Vill as the receiver (b)

To see the event more clearly, though, we can focus on one specific receiver (which will still yield multiple IPPs, as the receiver works with different satellites). For the particular case of the Villafranca, Spain station (identified as Vill), we obtain the plot from figure 4.1(b). At this time of the day around 11:00h the Sun would have a greater effect on the IPPs of this station, so the spike can be seen more clearly.

As mentioned before, the flare took place at 11.05, so we could proceed using the studied data range and this epoch in particular.

4.3 Solar-zenith angle

The solar-zenith angle (denoted χ from now onward) plays a major role when studying this event: it is the angle formed by the Sun and the Earth's zenith and indicates the effect the flare is having on a particular IPP. It is expected that this variable presents a correlation with the increase in VTEC, which is what we aim to observe in this chapter.

Figure **??**, at the end of the chapter, provides a visual representation of this variable that along with the results depicts how it can affect the VTEC value.

Obtaining the angle between two celestial objects has been shown in the previous section by means of equations 4.3, 4.4 and 4.5, when calculating the angle between the Sun and a detected GRB.

$$unitVectorObjectA = \begin{bmatrix} \cos\delta_g * \cos\alpha_g \\ \cos\delta_g * \sin\alpha_g \\ \sin\delta_g \end{bmatrix} \tag{4.3}$$

$$unitVectorObjectB = \begin{bmatrix} \cos\delta_s * \cos\alpha_s \\ \cos\delta_s * \sin\alpha_s \\ \sin\delta_s \end{bmatrix} \tag{4.4}$$

$$\cos\beta = unitVectorObjectA \cdot unitVectorObjectB \tag{4.5}$$

For this case, though, the angle is computed using the IPP's Right Ascension and Latitude (equivalent to declination), yielding the cosine of χ, the **solar-zenith angle**.

USING THE OTHER EQUIATION explain

The previous computation is done for every IPP (every line outputed by the AWK script) as shown in the following Fortran code:

```
subroutine traverseFile (raSun, decSun)
implicit none
  real :: raIPP, decIPP, mapIon, d2Li, cosX, vtec
  real, intent(in) :: raSun, decSun

  350 format  (F10.4, F10.4, F15.10, F15.10)

  do while (1 == 1)
    read (1, *, end = 240) raIPP, decIPP, mapIon, d2Li
    raIPP = toRadian(raIPP)
    decIPP = toRadian(decIPP)
    cosX = computeSolarZenithAngle(raIPP, decIPP, raSun, decSun)
    vtec = estimateVTEC(mapIon, d2Li)
    if (vtec < 0.4 .and. vtec > -0.4) then
      write (*, 350) cosX, vtec
    end if
  end do
  240 continue
end subroutine traverseFile
```

Listing 4.3: Reading the content of the file and storing the computations for plotting

We can also see in the previous code that VTEC values not inside the (-0.4, 0.4) range are discarded. This is a first, simple approach to discarding outliers, because we could visually see from the plots that most values stayed between those numbers.

The following code is the function that implements the equations 4.3, 4.4 and 4.5:

```
real function computeSolarZenithAngle (raIPP, decIPP, raSun, decSun)
      implicit none

      real, intent(in) :: raIPP, decIPP, raSun, decSun
      real :: solarZenithAngle

      solarZenithAngle = sin(decIPP)*sin(decSun) + cos(decIPP)*cos(decSun)*cos
    (raIPP - raSun)
      return
    end function computeSolarZenithAngle
```

Listing 4.4: Computation of the solar-zenith a angle

4.4 Results

Taking 212.338º and −13.060º as the Sun's right ascension and declination, respectively, and the measurements of all IPPs at 11.05 hours, figure 4.2 shows the plot of the output of our program.

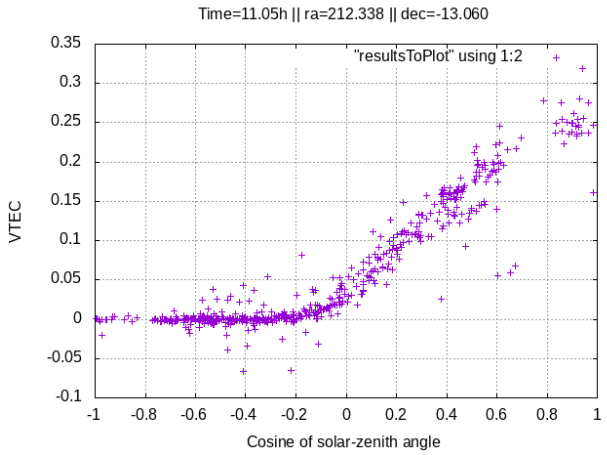

Figure 4.2: VTEC value as a function of the solar-zenith angle cosine

As we can observe, there is a strong relation between the cosine of the solar-zenith angle and the VTEC content, which increases from $\cos\chi = 0$ (90º) to $\cos\chi = 1$ (0º) and it doesn't seem to affect it from $\cos\chi = -1$ (180º) to $\cos\chi = 1$ (0º).

Visually this can be seen as follows:

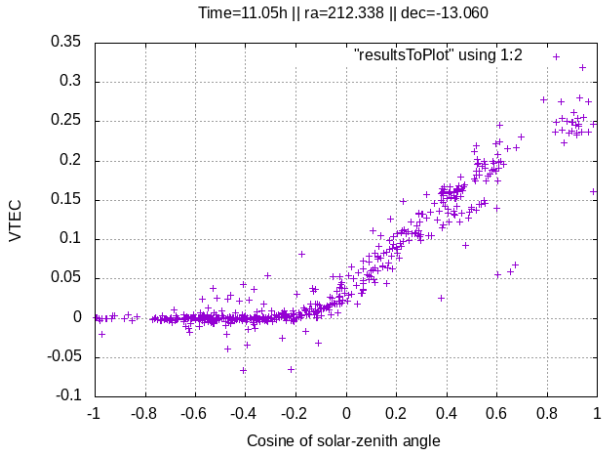

Figure 4.3: VTEC value as a function of the solar-zenith angle cosine

In conclusion, we can see that there appears to be correlation between the two variables. This correlation will be studied in more detail in the following section, where a first approach of the algorithm will be presented to detect the flare without knowing its location.

Chapter 5

Sun flare detection algorithm

Explain why brute force aproach

5.1 Key elements

5.1.1 Correlation

explain, formulas, references, etc

explain R and compare to show the computation is correct

5.1.2 Moment of the flare

The first part of the algorithm was, without going into the actual computations regarding the position of the IPPs, the possible Sun locations, etc, finding out when to perform the study, that is, detecting a spike in the VTEC content in general, for any IPP.

A first approach to detecting thiswe first wanted to detect a spike in the VTEC content throughout the day in a simple way. For each epoch [1] we computed the mean VTEC of all IPPs and inserted it into a priority queue. We did this because we wanted to see thbut a simple single-pass max-value finder would work

explicar buscar pico por hill climbing o algo asi usando la grafica de la distribucion. Al encontrar un momento exacto en el que centrarnos empezar a estudiar ahi

5.2 Brute force approach

explicar que es para entender que debemos hacer

5.2.1 Pseudocode

primero pseudocodigo, explicar for each dec for each ra

[1] In our data set the epochs ranged from 10.5 to 11.5, that it is, 10:30AM to 11:30AM with a sampling rate of 1/120 hours or 30 seconds

Algorithm 1 My algorithm

```
1: procedure MyProcedure
2:     stringlen ← length of string
3:     i ← patlen
4: top:
5:     if i > stringlen then return false
6:     j ← patlen
7: loop:
8:     if string(i) = path(j) then
9:         j ← j − 1.
10:        i ← i − 1.
11:        goto loop.
12:        close;
13:    i ← i + max(delta_1(string(i)), delta_2(j)).
14:    goto top.
```

entonces explicar aqui lo de los polos, in a first approach to this in which to visually see ourselves the differences between possible Sun positions we obtained a plot for each possibility (figure 5.1), we could see this happening:

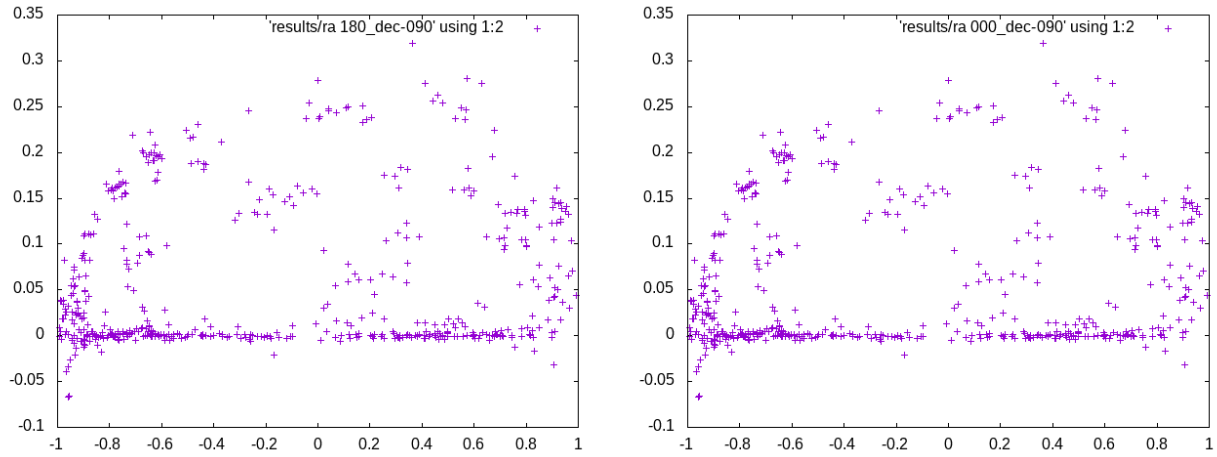

(a) ra180 and dec-090 (b) ra000 and dec-090

Figure 5.1: dasdasdasda

5.2.2 Linking C++ and Fortran

explicar aqui que la logica se hace con c++ y la computacion numerica con Fortran

```
import numpy as np

def incmatrix(genl1,genl2):
m = len(genl1)
```

```
n = len(genl2)
M = None #to become the incidence matrix
VT = np.zeros((n*m,1), int)  #dummy variable

#compute the bitwise xor matrix
M1 = bitxormatrix(genl1)
M2 = np.triu(bitxormatrix(genl2),1)

for i in range(m-1):
for j in range(i+1, m):
[r,c] = np.where(M2 == M1[i,j])
for k in range(len(r)):
VT[(i)*n + r[k]] = 1;
VT[(i)*n + c[k]] = 1;
VT[(j)*n + r[k]] = 1;
VT[(j)*n + c[k]] = 1;

if M is None:
M = np.copy(VT)
else:
M = np.concatenate((M, VT), 1)

VT = np.zeros((n*m,1), int)

return M
```

Listing 5.1: Python example

5.2.3 Results

```
[C++: Finding a spike in the VTEC distribution]
[AWK: Filtering all data by best epoch: 11.05]
[C++ -> Fortran: Finding the Person coefficients for possible Suns | Epoch =
    11.050000]
[C++ -> R: Computing correlation coefficient for each possible Sun with R]
[R: RESULTS]
Largest correlation coefficient: 0.9073422
Estimated Sun's location:  ra210_dec-010
```

Listing 5.2: Brute force approach algorithm output

testing [9] [14] [6]

Bibliography

[1] (Archived website) The Starlink Project. `https://web.archive.org/web/20120123062045/http://starlink.jach.hawaii.edu/starlink/WelcomePage`. [Online; accessed 10-March-2019].

[2] International GNSS Service Website. `http://www.igs.org/about`. [Online; accessed 8-March-2019].

[3] N. Crustal Dynamics Data Information System (CDDIS). Archive of Space Geodesy Data. `https://cddis.nasa.gov/`. [Online; accessed 29-March-2019].

[4] J. M. Dow, R. E. Neilan, and C. Rizos. The international GNSS service in a changing landscape of global navigation satellite systems. *Journal of geodesy*, 83(3-4):191–198, 2009.

[5] N. Gehrels, G. Chincarini, P. Giommi, K. Mason, J. Nousek, A. Wells, N. White, S. Barthelmy, D. Burrows, L. Cominsky, et al. The swift gamma-ray burst mission. *The Astrophysical Journal*, 611(2):1005, 2004.

[6] Goddard Space Flight Center (NASA). Swift GRBs Archive. `https://swift.gsfc.nasa.gov/archive/grb_table.html/`. [Online; accessed 1-March-2019].

[7] C. J. Hegarty and E. Chatre. Evolution of the Global Navigation Ssatellite System (GNSS). *Proceedings of the IEEE*, 96(12):1902–1917, 2008.

[8] M. Hernández-Pajares, A. García-Rigo, J. M. Juan, J. Sanz, E. Monte, and A. Aragón-Àngel. GNSS measurement of EUV photons flux rate during strong and mid solar flares. *Space Weather*, 10(12):1–16, 2012.

[9] M. Hernández-Pajares, J. Juan, J. Sanz, R. Orus, A. Garcia-Rigo, J. Feltens, A. Komjathy, S. Schaer, and A. Krankowski. The igs vtec maps: a reliable source of ionospheric information since 1998. *Journal of Geodesy*, 83(3-4):263–275, 2009.

[10] M. Hernández-Pajares, J. M. Juan, J. Sanz, À. Aragón-Àngel, A. García-Rigo, D. Salazar, and M. Escudero. The ionosphere: effects, gps modeling and the benefits for space geodetic techniques. *Journal of Geodesy*, 85(12):887–907, 2011.

[11] B. Hofmann-Wellenhof, H. Lichtenegger, and E. Wasle. *GNSS–global navigation satellite systems: GPS, GLONASS, Galileo, and more*. Springer Science & Business Media, 2007.

[12] Institute of Space Sciences (CSIC-IEEC. Magnetar Outburst Online Catalog. http://magnetars.ice.csic.es/#/parameters. [Online; accessed 3-March-2019].

[13] Jochen Greiner, Max-Planck-Institute for extraterrestrial Physics. GRB collection. http://www.mpe.mpg.de/~jcg/grbgen.html. [Online; accessed 3-March-2019].

[14] D. Martínez Cid. First study on the feasibility of stellar flares detection with gps. B.S. thesis, Universitat Politècnica de Catalunya, 2016.

[15] C. E. Noll. The crustal dynamics data information system: A resource to support scientific analysis using space geodesy. *Advances in Space Research*, 45(12):1421–1440, 2010.

[16] S. W. P. C. N. Oceanic and A. Administration). Ionosphere. https://www.swpc.noaa.gov/phenomena/ionosphere. [Online; accessed 25-March-2019].

[17] P. W. Roming, T. E. Kennedy, K. O. Mason, J. A. Nousek, L. Ahr, R. E. Bingham, P. S. Broos, M. J. Carter, B. K. Hancock, H. E. Huckle, et al. The swift ultra-violet/optical telescope. *Space Science Reviews*, 120(3-4):95–142, 2005.

[18] T. Singh, M. Hernandez-Pajares, E. Monte, A. Garcia-Rigo, and G. Olivares-Pulido. GPS as a solar observational instrument: Real-time estimation of EUV photons flux rate during strong, medium, and weak solar flares. *Journal of Geophysical Research: Space Physics*, 120(12):10–840, 2015.

[19] S. Solar Center. The Earth's Ionosphere. http://solar-center.stanford.edu/SID/activities/ionosphere.html. [Online; accessed 13-March-2019].

[20] Solar System Exploration, NASA Science. Reference Systems. https://solarsystem.nasa.gov/basics/chapter2-2/. [Online; accessed 5-March-2019].